

MULTIWAVELENGTH OBSERVATIONS OF THE TeV BINARY LS I +61° 303 WITH VERITAS, *Fermi*-LAT, AND *Swift*/XRT DURING A TeV OUTBURST

E. ALIU¹, S. ARCHAMBAULT², B. BEHERA³, K. BERGER⁴, M. BEILICKE⁵, W. BENBOW⁶, R. BIRD⁷, A. BOUVIER⁸, V. BUGAEV⁵,
 M. CERRUTI⁶, X. CHEN^{3,9}, L. CIUPIK¹⁰, M. P. CONNOLLY¹¹, W. CUI¹², J. DUMM¹³, A. FALCONE¹⁴, S. FEDERICI^{3,9}, Q. FENG¹²,
 J. P. FINLEY¹², P. FORTIN⁶, L. FORTSON¹³, A. FURNISS⁸, N. GALANTE⁶, G. H. GILLANDERS¹¹, S. GRIFFIN², S. T. GRIFFITHS¹⁵,
 J. GRUBE¹⁰, G. GYUK¹⁰, D. HANNA², J. HOLDER⁴, G. HUGHES³, T. B. HUMENSKY¹, P. KAARET¹⁵, M. KERTZMAN¹⁶, Y. KHASSEN⁷,
 D. KIEDA¹⁷, F. KRENNRICH¹⁸, M. J. LANG¹¹, G. MAIER³, P. MAJUMDAR^{19,20}, S. MCARTHUR²¹, A. MCCANN²², P. MORIARTY²³,
 R. MUKHERJEE¹, A. O’FAOLÁIN DE BHRÓITHE⁷, R. A. ONG¹⁹, A. N. OTTE²⁴, N. PARK²¹, J. S. PERKINS²⁵, M. POHL^{3,9}, A. POPKOW¹⁹,
 H. PROKOPH³, J. QUINN⁷, K. RAGAN², J. RAJOTTE², G. RATLIFF¹⁰, P. T. REYNOLDS²⁶, G. T. RICHARDS²⁴, E. ROACHE⁶,
 G. H. SEMBROSKI¹², F. SHEIDAEI¹⁷, C. SKOLE³, A. W. SMITH¹⁷, D. STASZAK², I. TELEZHINSKY^{3,9}, J. TYLER², A. VARLOTTA¹²,
 S. VINCENT³, S. P. WAKELY²¹, T. C. WEEKES⁶, A. WEINSTEIN¹⁸, R. WELSING³, A. ZAJCZYK⁵, AND B. ZITZER²⁷

¹ Physics Department, Columbia University, New York, NY 10027, USA

² Physics Department, McGill University, Montreal, QC H3A 2T8, Canada

³ DESY, Platanenallee 6, D-15738 Zeuthen, Germany

⁴ Department of Physics and Astronomy and the Bartol Research Institute, University of Delaware, Newark, DE 19716, USA

⁵ Department of Physics, Washington University, St. Louis, MO 63130, USA

⁶ Fred Lawrence Whipple Observatory, Harvard-Smithsonian Center for Astrophysics, Amado, AZ 85645, USA

⁷ School of Physics, University College Dublin, Belfield, Dublin 4, Ireland

⁸ Santa Cruz Institute for Particle Physics and Department of Physics, University of California, Santa Cruz, CA 95064, USA

⁹ Institute of Physics and Astronomy, University of Potsdam, D-14476 Potsdam-Golm, Germany

¹⁰ Astronomy Department, Adler Planetarium and Astronomy Museum, Chicago, IL 60605, USA

¹¹ School of Physics, National University of Ireland Galway, University Road, Galway, Ireland

¹² Department of Physics, Purdue University, West Lafayette, IN 47907, USA

¹³ School of Physics and Astronomy, University of Minnesota, Minneapolis, MN 55455, USA

¹⁴ Department of Astronomy and Astrophysics, 525 Davey Lab, Pennsylvania State University, University Park, PA 16802, USA

¹⁵ Department of Physics and Astronomy, University of Iowa, Van Allen Hall, Iowa City, IA 52242, USA

¹⁶ Department of Physics and Astronomy, DePauw University, Greencastle, IN 46135-0037, USA

¹⁷ Department of Physics and Astronomy, University of Utah, Salt Lake City, UT 84112, USA; aw.smith@utah.edu, sheidaei@physics.utah.edu

¹⁸ Department of Physics and Astronomy, Iowa State University, Ames, IA 50011, USA

¹⁹ Department of Physics and Astronomy, University of California, Los Angeles, CA 90095, USA

²⁰ Saha Institute of Nuclear Physics, Kolkata 700064, India

²¹ Enrico Fermi Institute, University of Chicago, Chicago, IL 60637, USA

²² Kavli Institute for Cosmological Physics, University of Chicago, Chicago, IL 60637, USA

²³ Department of Life and Physical Sciences, Galway-Mayo Institute of Technology, Dublin Road, Galway, Ireland

²⁴ School of Physics and Center for Relativistic Astrophysics, Georgia Institute of Technology, 837 State Street NW, Atlanta, GA 30332-0430, USA

²⁵ N.A.S.A./Goddard Space-Flight Center, Code 661, Greenbelt, MD 20771, USA

²⁶ Department of Applied Physics and Instrumentation, Cork Institute of Technology, Bishopstown, Cork, Ireland

²⁷ Argonne National Laboratory, 9700 S. Cass Avenue, Argonne, IL 60439, USA

Received 2013 July 12; accepted 2013 October 22; published 2013 November 26

ABSTRACT

We present the results of a multiwavelength observational campaign on the TeV binary system LS I +61° 303 with the VERITAS telescope array (>200 GeV), *Fermi*-LAT (0.3–300 GeV), and *Swift*/XRT (2–10 keV). The data were taken from 2011 December through 2012 January and show a strong detection in all three wavebands. During this period VERITAS obtained 24.9 hr of quality selected livetime data in which LS I +61° 303 was detected at a statistical significance of 11.9σ . These TeV observations show evidence for nightly variability in the TeV regime at a post-trial significance of 3.6σ . The combination of the simultaneously obtained TeV and X-ray fluxes do not demonstrate any evidence for a correlation between emission in the two bands. For the first time since the launch of the *Fermi* satellite in 2008, this TeV detection allows the construction of a detailed MeV–TeV spectral energy distribution from LS I +61° 303. This spectrum shows a distinct cutoff in emission near 4 GeV, with emission seen by the VERITAS observations following a simple power-law above 200 GeV. This feature in the spectrum of LS I +61° 303, obtained from overlapping observations with *Fermi*-LAT and VERITAS, may indicate that there are two distinct populations of accelerated particles producing the GeV and TeV emission.

Key words: acceleration of particles – binaries: general – gamma rays: stars – relativistic processes – X-rays: binaries

1. INTRODUCTION

The high-mass X-ray binary LS I +61° 303 is perhaps the most studied member of a surprisingly small class of X-ray binary systems which are also known sources of TeV emission. Despite many years of observations across the electromagnetic spectrum, the system remains, in some respects, poorly characterized. Known to be the pairing of a massive B0 Ve star

and a compact object of unknown nature (Casares et al. 2005; Hutchings & Crampton 1981), LS I +61° 303 has been known historically for its energetic outbursts at radio, X-ray, GeV, and TeV wavelengths (Abdo et al. 2009a; Acciari et al. 2008; Albert et al. 2006; Gregory 2002; Greiner & Rau 2001; Harrison et al. 2000; Zhang et al. 2010), all of these showing correlation with the 26.5 day orbital cycle of the compact object. Radial velocity measurements show the orbit to be

elliptical ($e = 0.537 \pm 0.034$), with periastron passage occurring around phase $\phi = 0.275$, apastron passage at $\phi = 0.775$, superior conjunction at $\phi = 0.081$, and inferior conjunction at $\phi = 0.313$ (Aragona et al. 2009). Although it should be noted that all of the orbital parameters of LS I +61° 303 are subject to some uncertainty as the inclination of the system is not precisely known.

Observations in the non-thermal regime have managed to illustrate some key phenomena. Extensive observations by both *RXTE* and *Swift*/XRT have provided a wealth of X-ray data which show a regular emission period consistent with the orbital period (Smith et al. 2009; Esposito et al. 2007). The modulation of this X-ray peak is seen on multiple timescales, from individual orbits up to several years; most importantly, a modulation on a ~ 4.5 yr timescale (Li et al. 2012; Chernyakova et al. 2012) has been observed in the hard X-ray band, reminiscent of the well known 4.5 yr modulation of the radio period (Gregory 2002). However, a definitive link between the particle acceleration processes producing the radio emission and those producing the X-ray emission is still lacking. An additional feature of the system is the possible association of short (< 0.1 s), high luminosity X-ray bursts from the system (de Pasquale et al. 2008; Burrows 2012) which have been interpreted as the result of the emission from a high magnetic field neutron star (Papitto et al. 2012). Further observations of such behavior from the system in the X-ray band, definitively linked to LS I +61° would solidify this association.

In the GeV band, LS I +61° 303 was one of the few non-pulsar galactic objects firmly identified in the initial *Fermi*-LAT Bright Source List with an average flux of $(0.82 \pm 0.03_{\text{stat}} \pm 0.07_{\text{sys}}) \times 10^{-6} \text{ } \gamma \text{ cm}^{-2} \text{ s}^{-1}$ above 100 MeV (Abdo et al. 2009a). The spectrum showed an exponential cutoff at $6.3 \pm 1.1_{\text{stat}} \pm 0.4_{\text{sys}}$ GeV and a photon index of $\Gamma = 2.21 \pm 0.04_{\text{stat}} \pm 0.06_{\text{sys}}$. In the first 8 months of LAT data, the source demonstrated a clear modulation of GeV emission with a period of ~ 26.5 days, compatible with the radio period. The highest GeV fluxes were measured around phase $\phi = 0.4$, close to periastron. However, subsequent analysis of ~ 4.5 yr of *Fermi*-LAT data shows clear evidence for long term variability of the mean orbital flux along with the apparent disappearance of its previously observed orbital modulation (Hadasch et al. 2012). This long term variability has recently been elucidated in Ackermann et al. (2013), where the *Fermi*-LAT Collaboration shows a detection of the ~ 4.5 yr modulation of the GeV flux around apastron, consistent with the modulation seen in both radio and X-rays.

As a TeV source, the system has presented puzzling behavior. Initial detections in 2006–2007 by both the VERITAS and MAGIC collaborations (Albert et al. 2006; Acciari et al. 2008) over many orbital cycles showed the source to be a variably bright TeV source, with emission peaking around apastron passage. Subsequent observations in 2008–2010 (Acciari et al. 2011) showed no evidence for emission during these previously detected phases, instead only detecting the source at a lower TeV flux near the periastron passage of a single orbit. The connection between the observed emission in different energy bands is not clear; initial detections of a correlation between the TeV and X-ray fluxes (Anderhub et al. 2009) were not seen in later observations. Additionally, previous observations have not shown the GeV and TeV emission from the system to be strongly correlated either (Acciari et al. 2011).

As is the case with many TeV sources, the models to explain observed emission consist of both leptonic (inverse

Compton scattering) and hadronic (pion decay resulting from relativistic proton interactions) variations. LS I +61° 303 is certainly no different in this respect, however, the confusion between emission models is compounded by an ambiguity in what type of engine actually powers the particle acceleration. LS I +61° 303 was originally thought to be a microquasar system due to the observation of what appeared to be extended radio jets (Massi et al. 2001). In this scenario, emission from the system is powered by a variably fed accretion disk which, in turn, powers a relativistic jet. The variability observed across the spectrum would then be explained by the accretion disk's exposure to varying levels of the strong stellar wind common to Be star systems. This model (under the assumption of basic Bondi–Hoyle accretion) would then predict non-thermal emission in the various bands to be coupled (in the simplest scenario) with the maximum flux occurring near periastron passage where the density of the stellar material is greatest. While this appears to be true sometimes in the GeV regime, it is not true in the TeV regime where emission is typically at a maximum near apastron passage.

However, the existence of a radio jet (and the validity of using a microquasar scenario) was called into question by high resolution Very Long Baseline Array imaging which observed what appeared to be the cometary emission from the interaction between a pulsar wind and the wind of the stellar companion (Dhawan et al. 2006). In this scenario (where the emission is powered by a shock front between the two winds) the variability would also result from varying levels of stellar wind density. However, in this model the emission in the various bands is decoupled by both the magnetic field strength at the shock and “stand off distance” (distance from the shock to the pulsar) changing as function of orbit. The change in these two quantities would dictate both cooling mechanisms and acceleration parameters, thus changing the relative intensities of emission between bands.

It should be pointed out that neither of these models can explain all of the observed emission variability in the system (for instance, the VERITAS detection of TeV emission far away from apastron passage). Additionally, since neither pulsations nor an accretion-like X-ray spectrum have yet to be observed in the system, current observations have not yielded a definitive answer to whether the system harbors a pulsar or black hole and both theoretical frameworks used to describe this system are still lacking strong constraints. What is clear, however, is that the simplest version of either model will not adequately explain the observations. For example, both photon–photon absorption and line-of-sight effects almost certainly have to be taken into account when accounting for the observed variability. For examples of more recently advanced observations and models, see Zabalza et al. (2013), Torres et al. (2012; binary pulsar model), and Zimmerman & Massi (2012; microquasar model).

Determining the correct physical model for this source requires additional dedicated observations across the multiwavelength spectrum. In this work we detail the multiwavelength campaign on LS I +61° 303 incorporating both contemporaneous and simultaneous observations in the X-ray (*Swift*/XRT), GeV (*Fermi*-LAT), and TeV (VERITAS) regimes. This campaign was taken during a relatively strong period of emission in the TeV regime, and stands as the first time that simultaneous GeV/TeV have been available during a high TeV state. During this high state, VERITAS detected marginal evidence for nightly variability in the system as well as a lack of strong correlated emission between the TeV flux and X-ray/GeV fluxes.

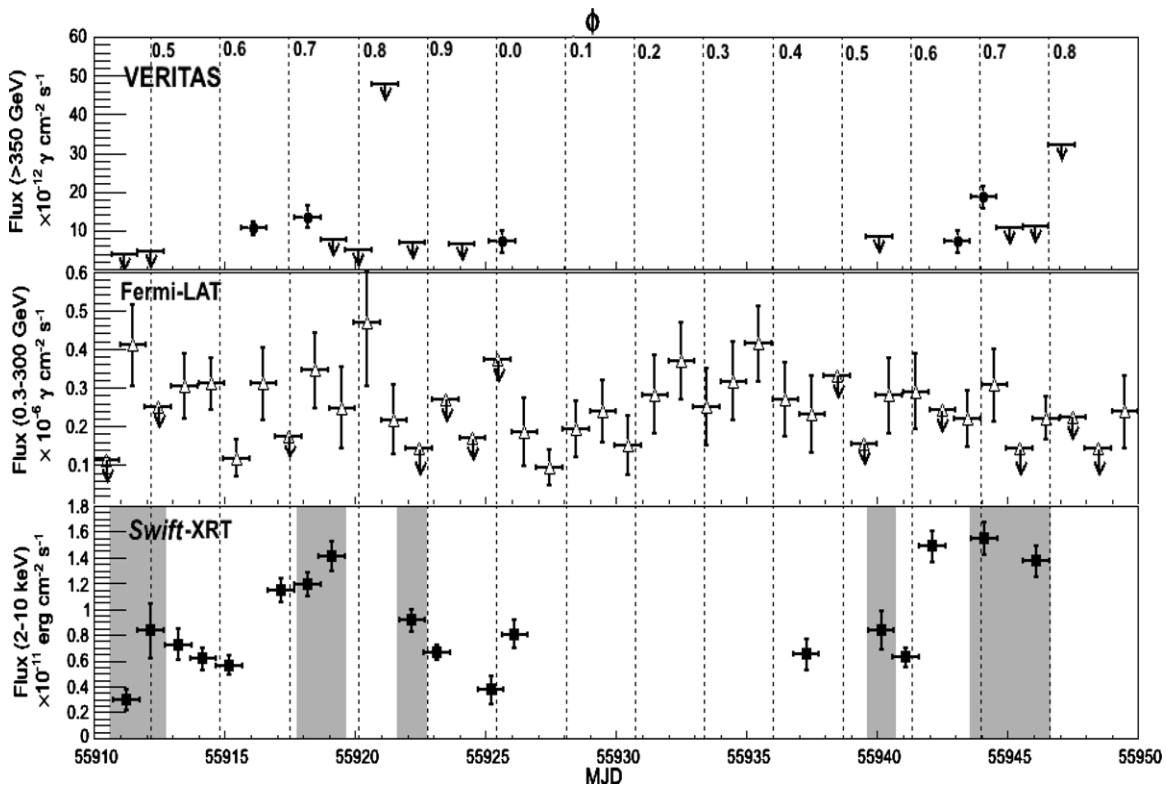


Figure 1. VERITAS (>350 GeV daily integrations, top), *Fermi*-LAT (0.3–300 GeV, middle), and *Swift*/XRT (0.3–10 keV, bottom) light curves for LS I +61° 303 during 2011 December–2012 February. The data is also shown as a function of orbital phase (ϕ). VERITAS 99% flux upper limits are shown for points with $<3\sigma$ significance and are represented by arrows. *Fermi*-LAT upper limits (90% confidence level) are also shown by arrows. The gray shaded regions represent the observations obtained simultaneously which are used for the X-ray/TeV correlation studies in this work.

Additionally, the spectral energy distribution (SED) obtained during these observations reveals a puzzling lack of detected emission between 30 and 200 GeV which makes the characterization of the gamma-ray emission non-trivial.

2. VERITAS OBSERVATIONS

The VERITAS array (Holder et al. 2008) of imaging atmospheric Cherenkov telescopes (IACTs), located in southern Arizona (1.3 km a.s.l., 31°40′30″ N, 110°57′07″ W), began four-telescope array observations in 2007 September. The array is composed of four 12 m diameter telescopes, each with a Davies-Cotton tessellated mirror structure of 345 12 m focal length hexagonal mirror facets (total mirror area of 110 m²). Each telescope focuses Cherenkov light from particle showers onto its 499-pixel photomultiplier tube camera. Each pixel has a field of view of 0°15, resulting in a camera field of view of 3°5. VERITAS has the capability to detect and measure gamma rays in the 100 GeV to 30 TeV energy regime with an energy resolution of 15%–20% and an angular resolution of $<0^{\circ}.1$ on an event by event basis.

VERITAS observed LS I +61° 303 beginning in early 2011 December (MJD 55911) until late 2012 January (MJD 55497), acquiring a total of 24.5 hr of quality selected, live-time observations. These observations provided detailed (although uneven) sampling of the phase bins $\phi = 0.45$ – 0.05 of the binary orbit. Figure 1 shows the source light curve binned by both MJD and orbital phase. During the orbital phase regions of 0.5–0.8, the source was highly active, presenting a flux of 5 – $15 \times 10^{-12} \gamma \text{ cm}^{-2} \text{ s}^{-1}$ above 350 GeV, or approximately 5%–15% of the Crab Nebula flux in the same energy regime. For the entire 24.5 hr observation, VERITAS detected an

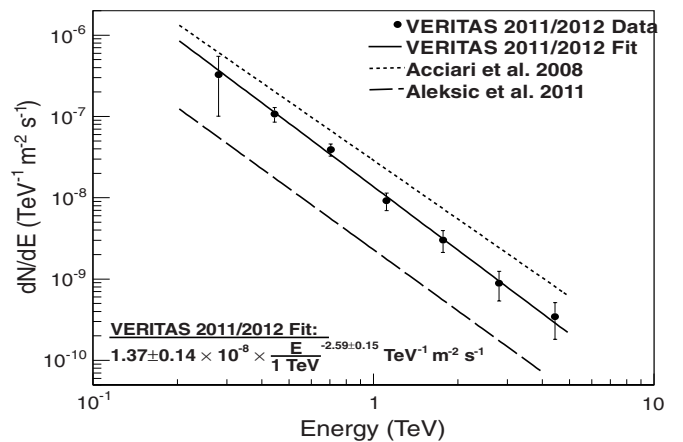


Figure 2. VERITAS SED obtained from the 2011/2012 observations. We also show the SED power-law fit to both higher (Acciari et al. 2008) and lower (Aleksic et al. 2012) flux states of the source.

excess of 791 events from LS I +61° 303, equivalent to a detection at the 11.9σ significance level. The data are used to create a differential energy spectrum from 0.2 to 5 TeV which is reasonably fit by a power-law ($\chi^2/\text{n.d.f} = 1.1/5$) described by $(1.37 \pm 0.14_{\text{stat}}) \times 10^{-12} \times ((E/1 \text{ TeV}))^{-2.59 \pm 0.15_{\text{stat}}} \gamma \text{ s TeV}^{-1} \text{ cm}^{-2} \text{ s}^{-1}$. A comparison of this spectrum with those obtained by previous measurements at different flux levels (Aleksic et al. 2012; Acciari et al. 2008) shows no indication for variability in the spectral slope from the source across a wide range of flux levels (see Figure 2).

The observations of LS I +61° 303 taken in 2011 also display an indication that the source may be variable in the TeV regime

Table 1

The Probabilities for Both the Flux Increase and Decrease per Each Pair of Nightly Separated Fluxes

MJD	Flux (>350 GeV) $\times 10^{-12} \gamma \text{ s cm}^{-2} \text{ s}^{-1}$	$p(F_1 > F_2) (\sigma)$	$p(F_2 > F_1) (\sigma)$
55911	-1.5 ± 1.8	$<10^{-5} (<0.1\sigma)$	
55912	-1.02 ± 2.0		0.18 (0.23 σ)
55918	13.5 ± 2.8	0.99 (2.72σ)	
55919	3.7 ± 1.3		$<10^{-5} (<0.1\sigma)$
55919	3.7 ± 1.3	0.76 (1.17 σ)	
55920	-0.77 ± 2.0		$<10^{-5} (<0.1\sigma)$
55920	-0.77 ± 2.0	$3.9 \times 10^{-3} (<0.1\sigma)$	
55921	-1.02 ± 2.0		$7.6 \times 10^{-4} (<0.1\sigma)$
55924	1.3 ± 1.8	$<10^{-5} (<0.1\sigma)$	
55925	7.2 ± 2.8		0.69 (1.01 σ)
55943	18.6 ± 3.3	$1.6 \times 10^{-3} (<0.1\sigma)$	
55944	18.6 ± 2.8		$1.9 \times 10^{-3} (<0.1\sigma)$
55944	18.6 ± 2.8	0.99 (3.57σ)	
55945	4.8 ± 2.1		$<10^{-5} (<0.1\sigma)$
55945	4.8 ± 2.1	$7.4 \times 10^{-3} (<0.1\sigma)$	
55946	4.1 ± 2.4		$4.0 \times 10^{-4} (<0.1\sigma)$
55946	4.1 ± 2.4	$<10^{-5} (<0.1\sigma)$	
55947	13.7 ± 5.9		0.47 (0.63 σ)

Note. All probabilities shown are post-trials, accounting for nine trials (nine pairs of fluxes). All errors quoted are statistical only.

on a timescale much shorter than previously observed. While LS I+61° 303 is known to be a variable TeV source on the timescale of a single orbital period, the 2011 VERITAS observations indicate that the source may be variable on a nightly timescale. To test this hypothesis, we proceed by collecting the nightly absolute fluxes (Figure 1) and finding the pairs of observations which are separated by one day. Nine such pairs of observations exists within the 2011 observations and their fluxes are shown in Table 1. To test for variability on a nightly timescale we choose to test against the null hypothesis that, given a pair of nightly separated fluxes (F_1, F_2), F_2 was significantly larger than F_1 (as well as the inverse hypothesis). Assuming that both the source fluxes and errors are normally distributed, we construct the two-dimensional Gaussian function:

$$G(x, y) = \frac{1}{2\pi\sigma_1\sigma_2} e^{-\frac{(x-F_1)^2}{2\sigma_1^2} - \frac{(y-F_2)^2}{2\sigma_2^2}} \quad (1)$$

where σ represents the errors on the measured fluxes, and x and y are both flux space variables. Within this parameterization, a constant flux from night to night is represented by the function $y = x$. The probabilities that F_2 was greater than F_1 (or vice versa) can then be obtained by examining the integral:

$$\int_{-\infty}^{+\infty} dx \int_x^{+\infty} G(x, y) dy. \quad (2)$$

The resulting probabilities for $F_1 >, <F_2$ (Table 1) show marginal evidence that the source is variable on a nightly timescale. The observations taken on MJD 55918/55919 and MJD 55944/55945 show evidence for a flux decrease at the 2.7σ and 3.6σ significance level respectively. These significances are post-trials, accounting for nine trials (one trial for each nightly pair tested). We note that this analysis does not search for evidence of variability at any timescales other than the nightly

timescale. The flux differences present evidence for the TeV flux falling on a nightly timescale. However, we did not observe an increase in TeV flux on this same short timescale.

3. MULTIWAVELENGTH DATA

3.1. *Swift*/XRT

The *Swift*/XRT data (Burrows et al. 2005) were reduced using the HEASoft 6.12 package. Event files are calibrated and cleaned following the standard filtering criteria using the xrtpipeline task and applying the most recent *Swift*/XRT calibration files. All data were taken in photon counting mode, with grades 0–12 selected over the energy range 0.3–10 keV. Since the count rate was below 0.5 counts s^{-1} for all data, no evidence for photon pile-up in the core of the point-spread function (PSF) is evident. The source events are extracted from a circular region of radius of 30 pixels (47.2 arcsec). Background counts are extracted from a 40 pixel radius circle in a source-free region. Ancillary response files are generated using the xrtmkarf task, with corrections applied for the PSF losses and CCD defects. The latest response matrix from the XRT calibration files is applied. To ensure valid χ^2 minimization statistics during spectral fitting, the extracted XRT energy spectra are rebinned to contain a minimum of 20 counts in each bin. Spectral analysis is performed with XSPEC 12.7. An absorbed power-law model, including the phabs model for the photoelectric absorption, is fit to each spectrum. A fixed column density is applied with an N_H of $6.1 \times 10^{21} \text{ cm}^{-2}$ (Rea et al. 2010). The spectral index of the source varied from -2.5 to -1.1 with reduced χ^2 values ranging from 0.2 to 1.6. As observed in Smith et al. (2009), the data show evidence for a correlation between the spectral index of the source and the 0.2–10 keV flux, with a Pearson correlation coefficient derived of 0.8 ± 0.1 .

The overall *Swift*/XRT light curve was extracted in the energy range of 2–10 keV and is shown in Figure 1. There were eight *Swift*/XRT observations that were taken simultaneously with VERITAS data (shown by gray bars in Figure 1). In order to compare the VERITAS flux measurements with previous X-ray–TeV correlation studies, the 350 GeV fluxes were interpolated to 300 GeV fluxes using the fitted spectral index of -2.59 derived from the current observations. Both the VERITAS/*Swift* observations taken in 2011/2012 as well as archival VERITAS and MAGIC measurements (Acciari et al. 2011) are shown in Figure 3. The correlation factor derived from the 2011/2012 observations was 0.36 ± 0.32 , consistent with two uncorrelated datasets. Including all simultaneous X-ray/TeV pointings from VERITAS and MAGIC results in a correlation coefficient of 0.33 ± 0.14 , which is consistent with no correlation.

3.2. *Fermi*-LAT

Fermi-LAT (Atwood et al. 2009) analysis was performed on all available photons in the 0.3–300 GeV band obtained between 2011 December 1 (MJD 55896) and 2012 February 1 (MJD 55958), in order to overlap as closely as possible with the VERITAS observations. The data were analyzed using Science Tools version v9r31p1, available from the Fermi Science Support Center (FSSC).²⁸ Standard data quality cuts for Pass 7 event reconstruction were applied as recommended by the FSSC, with only “source” (class 2) events being used for analysis. Other standard cuts were also applied (e.g., zenith

²⁸ <http://fermi.gsfc.nasa.gov/ssc/>

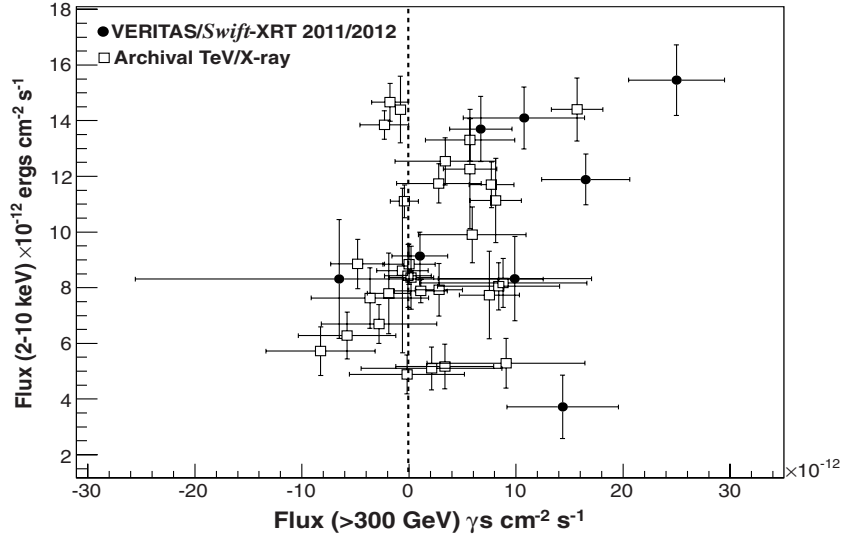


Figure 3. Comparison of the strictly simultaneous *Swift*/XRT and VERITAS data points. The data shows a correlation coefficient of 0.36 ± 0.32 , consistent with two uncorrelated data sets.

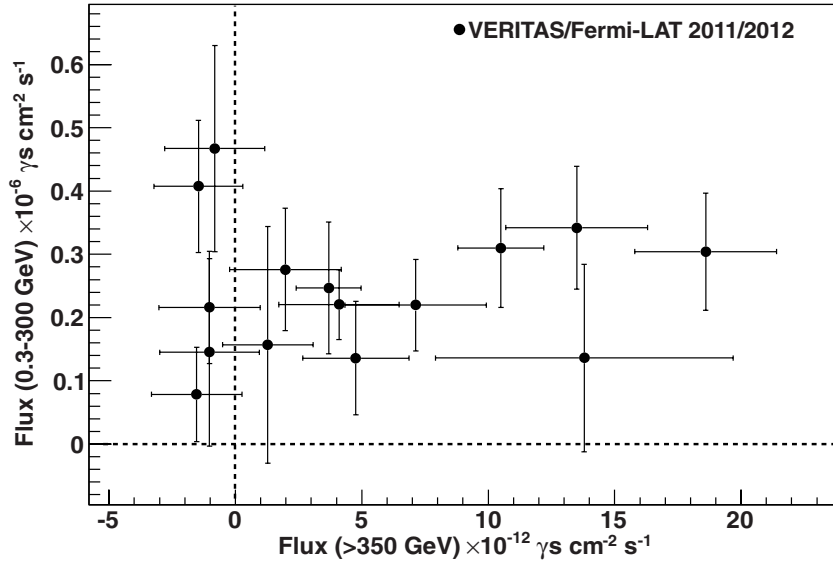


Figure 4. Comparison of nightly VERITAS and *Fermi*-LAT flux points. Analysis of the data results in a correlation coefficient of 0.1 ± 0.3 , consistent with two independent data sets.

angle larger than 100° in order to reduce the contamination from atmospheric secondary gamma rays from near the Earth's limb Abdo et al. 2009b).

The LAT light curve was produced using the python likelihood tools and scripts available from the FSSC.²⁹ A region of interest (ROI) of 10° was chosen and a model file incorporating all 2FGL sources within a region of 15° was used for the initial fit. In this fit, all source showing a test statistic (TS) value of less than 1 for the data interval chosen were excluded. Additionally, all source more than 5° from the center of the ROI had fixed parameters in the model fitting. The resulting model was used to produce the daily binned lightcurve (shown in Figure 1), by fixing all 2FGL source model parameters (with the exception of LS I +61° 303 and the nearby pulsar 2FGL J0248.1+6021). To test for any correlation between the GeV and TeV flux, a correlation coefficient between the overlapping observations is

calculated, with a coefficient of $r = 0.1 \pm 0.3$, consistent with two uncorrelated datasets (see Figure 4).

For spectral analysis, a binned maximum-likelihood method (gtlike) was used with an energy dependent ROI ranging from 2° to 10° . In order to determine the background, the 2FGL catalog (Nolan et al. 2012) was used to account for the emission from all sources within a radius ranging between 3° to 15° (also a function of energy). The spectrum is satisfactorily fit (reduced χ^2 value of 1.97 with 5 degrees of freedom) by a power law with exponential cutoff of the form $A \times (E/1 \text{ MeV})^{-\Gamma} \times \exp^{-(E/E_{\text{cutoff}})}$, with $A = (2.5 \pm 0.9) \times 10^{-4} \text{ } \gamma \text{ s MeV}^{-1} \text{ cm}^{-2} \text{ s}^{-1}$, $\Gamma = 2.13 \pm 0.06$, and $E_{\text{cutoff}} = 3.98 \pm 0.42 \text{ GeV}$ (see Figure 5). When comparing this spectrum to the one observed by VERITAS during contemporaneous observations, it is clear that the emission seen by *Fermi*-LAT experiences a dramatic fall off that is not observed in the TeV regime (see Figure 5). Since VERITAS observed the source at relatively large zenith angles (30° – 35°), the energy threshold of

²⁹ <http://fermi.gsfc.nasa.gov/ssc/data/analysis/user/>

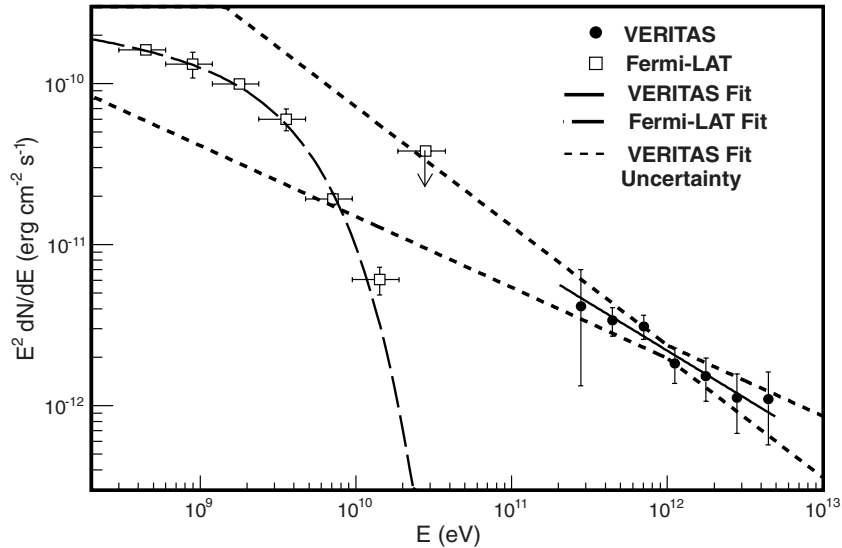


Figure 5. VERITAS and *Fermi*-LAT spectral energy distribution.

the TeV observations do not allow for a detailed examination of the 100–200 GeV energy range.

4. SUMMARY AND DISCUSSION

We have presented the results of a comprehensive multi-wavelength campaign of the TeV binary LS I +61° 303 using VERITAS, *Swift*/XRT, and *Fermi*-LAT observations. The source was detected strongly in the TeV regime while not showing a significant correlation with the observed emission in the X-ray or MeV–GeV regimes. The VERITAS differential energy spectrum obtained from these observations is well fit by a power law with spectral index consistent with previously published observations. The combination of the differential energy spectra obtained by both *Fermi*-LAT and VERITAS during the same time period reveals a puzzling lack of detected emission in the 1–200 GeV range. While the observation of this apparent discontinuity is not new (for example, Hadasch et al. 2012) the previous GeV–TeV multi wavelength SEDs of LS I +61° 303 have, up until now, been constructed with data taken from various epochs. The observations detailed here represent the first time that a contemporaneous SED has been constructed with *Fermi*-LAT and IACTs since the launch of *Fermi* in 2008. The distinctive cutoff seen in the *Fermi*-LAT data, coupled with the significant detection of emission in the >200 GeV VERITAS energy range during the contemporaneous observations detailed in this work indicate that the observed emission in the *Fermi*-LAT/VERITAS energy ranges is produced by two separate populations of particles. While we allow for the possibility that short term spectral variability in the *Fermi*-LAT energy regime could, in principle, produce a direct connection to the VERITAS TeV points, we consider such behavior unlikely given the spectral stability of the source in the *Fermi*-LAT regime (Abdo et al. 2009a).

Given that the GeV spectral cutoff observed in LS I +61° 303 is strongly reminiscent of the typical cutoff shape seen in known *Fermi*-LAT pulsars, it is natural to suspect that emission in the system is indeed powered by an energetic pulsar. This model, as first proposed in Maraschi & Treves (1981) and later developed and modeled in detail by Dubus (2006), explains the observed gamma-ray emission in LS I +61° 303

(as well as other known TeV binaries such as LS 5039 and PSR B1259-63) as being produced by the rotation power of a young pulsar. The inclusion of a pulsar in the system allows for much more flexibility in producing disparate populations of energetic particles (as appears to be observationally required in systems such as LS I +61° 303 and LS 5039) as there can be multiple acceleration regions for GeV/TeV energy particles: the inner pulsar magnetosphere, the shock interface between the pulsar and stellar winds (as well as multiple shocks separated by a contact discontinuity, as in Bednarek 2011), acceleration within the pulsar wind zone (Sierpowska-Bartosik & Torres 2008), and potentially Coriolis effect generated shock fronts on scales much larger than the binary system (i.e., Zabalza et al. 2013).

If we assume that the TeV emission is produced in the shock interaction between the two winds, and that the GeV emission is produced in a second acceleration region or different seed particles, then it is possible that the GeV emission might be produced in the inner regions of the pulsar magnetosphere. The observed GeV variability could then be explained by absorption effects as the pulsar travels through the varying stellar wind density of the Be star. This would offer a natural explanation for the lack of GeV emission in the arguably similar TeV binary system HESS J0632+057; the pulsar beam in that system could be pointed away from our line of sight. Bednarek (2011) argues against the pulsar magnetosphere being the source of the GeV emission in the GeV/TeV binary systems, citing the lack of GeV emission from PSR B 1259-63 away from periastron where absorption effects should not play a strong role. This is indeed true and would necessitate a different mechanism for GeV emission in PSR B1259-63; however, given the relative uncertainty in the various physical parameters of the known TeV binaries, it is entirely possible that different mechanisms for emission could be at work in the different binary systems.

The identification of LS I +61° 303 as a binary pulsar system is certainly not clear. For instance, despite many extensive searches Cañella et al. (2012); McSwain et al. (2011), no pulsations have ever been detected, although it is possible that the dense stellar environment of LS I +61° 303 might preclude such a detection.

The observations presented here also reveal the first strong evidence (99.97% confidence) for nightly variability in the source.

If confirmed, this variability can provide crucial constraints on the size of the TeV emission region (i.e., the size of possible “clumps” in the wind for pulsar binary models). Fast variability (\sim second timescale) has already been associated with LS I +61° 303 in the X-ray regime (Smith et al. 2009; Torres et al. 2010), limiting the size of the X-ray emission region. Given the source strength of LS I +61° 303 and current sensitivity of IACT arrays, it is unlikely that such fast variability will be observed by the current generation of TeV instruments, even if occurring in the source. However, if the TeV and X-ray emission have a common mechanism, it could be possible to observe variability in the system on the order of tens of minutes during TeV flaring episodes.

These observations, taken in the context of past observations with VERITAS and MAGIC, also bring up the issue of the possible long-term variability seen in the system. Observations of this system with TeV instruments have only been taking place since 2006; while the observations have not been dense enough to make strong statements about the long term behavior of the source, it would appear that the source may go through a long-term modulation in the high energy regime. The source was a strong TeV source in 2006/7 (Acciari et al. 2008; Albert et al. 2006); however, its TeV flux appears to have decreased over the succeeding years (Acciari et al. 2011; Aleksic et al. 2012). The “normal” apastron TeV emission was markedly quiet, while the source was sporadically detected at near-periastron phases. The VERITAS observations taken in 2011/2012 indicate that the source may have returned to its “normal” emission mode, with strong emission seen near apastron. Further long term observations of LS I +61° 303 with TeV instruments are key to understanding the possible multiyear modulation of the source and (given the lack of detected correlation between TeV emission and other bands) whether or not it is tied to similar emission modulation in radio (Gregory 2002), X-ray (Li et al. 2012; Chernyakova et al. 2012) and GeV gamma-rays (Ackermann et al. 2013).

This research is supported by grants from the U.S. Department of Energy Office of Science, the U.S. National Science Foundation and the Smithsonian Institution, by NSERC in Canada, by Science Foundation Ireland (SFI 10/RFP/AST2748) and by STFC in the U.K. We acknowledge the excellent work of the technical support staff at the Fred Lawrence Whipple Observatory and at the collaborating institutions in the construction and operation of the instrument. We thank the Swift Team for

scheduling contemporaneous observations and providing data and analysis tools. The authors would also like to thank Jeremy Perkins for his tireless assistance with *Fermi*-LAT data analysis.

REFERENCES

- Abdo, A., Ackermann, M., Ajello, M., et al. 2009a, *ApJL*, **701**, L123
 Abdo, A. A., Ackermann, M., Ajello, M., et al. 2009b, *PhRvD*, **80**, 122004
 Acciari, V., Aliu, E., Arlen, T., et al. 2011, *ApJ*, **738**, 3
 Acciari, V., Beilicke, M., Blaylock, G., et al. 2008, *ApJ*, **679**, 1427
 Ackermann, M., Ajello, M., Ballet, J., et al. 2013, *ApJL*, **773**, L35
 Albert, J., Aliu, E., Anderhub, H., et al. 2006, *Sci*, **312**, 1771
 Anderhub, H., Antonelli, L. A., Antoranz, P., et al. 2009, *ApJL*, **706**, L27
 Aleksic, J., Alvarez, E. A., Antonelli, L. A., et al. 2012, *ApJ*, **746**, 80
 Aragona, C., McSwain, M. V., Grundstrom, E. D., et al. 2009, *ApJ*, **698**, 514
 Atwood, W., Abdo, A. A., Ackermann, M., et al. 2009, *ApJ*, **697**, 1071
 Bednarek, W. 2011, *MNRAS*, **418**, L49
 Burrows, D. 2012, *GCN*, 12914, 1
 Burrows, D., Hill, J. E., Nousek, J. A., et al. 2005, *SSRv*, **120**, 165
 Cañella, A., Joshi, B. C., Paredes, J. M., et al. 2012, *A&A*, **543**, 122
 Casares, J., Ribas, I., Paredes, J. M., Martí, J., & Allende Prieto, C. 2005, *MNRAS*, **360**, 1105
 Chernyakova, M., Neronov, A., Molkov, S., et al. 2012, *ApJL*, **747**, L29
 de Pasquale, M., Barthelmy, S. D., Baumgartner, W. H., et al. 2008, *GCN*, **8209**, 1
 Dhawan, V., et al. 2006, in *Proc. of Microquasars and Beyond: From Binaries to Galaxies*, in *Proceedings of Science*, Como, IT, ed. T. Belloni, 52
 Dubus, G. 2006, *A&A*, **456**, 801
 Esposito, P., Caraveo, P. A., Pellizzoni, A., et al. 2007, *A&A*, **474**, 575
 Gregory, P. 2002, *ApJ*, **525**, 427
 Greiner, J., & Rau, A. 2001, *A&A*, **375**, 145
 Hadasch, D., Torres, D. F., Tanaka, T., et al. 2012, *ApJ*, **749**, 1
 Harrison, F., Ray, P. S., Leahy, D. A., Waltman, E. B., & Pooley, G. G. 2000, *ApJ*, **528**, 454
 Holder, J., Acciari, V. A., Aliu, E., et al. 2008, in *AIP Conf. Ser.* 1085, *High Energy Gamma-Ray Astronomy* (Melville, NY: AIP), **657**
 Hutchings, J., & Crampton, D. 1981, *PASP*, **93**, 486
 Li, J., Torres, D. F., Zhang, S., et al. 2012, *ApJL*, **744**, L13
 Maraschi, L., & Treves, A. 1981, *MNRAS*, **194**, 1
 Massi, M., Ribó, M., Paredes, J. M., Peracaula, M., & Estalella, R. 2001, *A&A*, **376**, 217
 McSwain, M. V., Ray, P. S., Ransom, S. M., et al. 2011, *ApJ*, **738**, 105
 Nolan, P., Abdo, A. A., Ackermann, M., et al. 2012, *ApJS*, **199**, 31N
 Papitto, A., Torres, D. F., & Rea, N. 2012, *ApJ*, **756**, 188
 Rea, N., Torres, D. F., van der Klis, M., et al. 2010, *MNRAS*, **405**, 2206
 Sierpowska-Bartosik, A., & Torres, D. 2008, *Aph*, **30**, 239
 Smith, A., Falcone, A., Holder, J., et al. 2009, *ApJ*, **693**, 1621
 Torres, D., Rea, N., & Esposito, P. 2012, *ApJ*, **744**, 106
 Torres, D., Zhang, S., Li, J., et al. 2010, *ApJL*, **719**, L104
 Zabalza, V., Bosch-Ramon, V., Aharonian, F., & Khangulyan, D. 2013, *A&A*, **551**, A13
 Zhang, S., Torres, D. F., Li, J., et al. 2010, *MNRAS*, **408**, 642
 Zimmerman, L., & Massi, M. M. 2012, *A&A*, **537**, 82